Agricultural and Forest Meteorology, 48 (1989) 185–199
Elsevier Science Publishers B.V., Amsterdam — Printed in The Netherlands

THE MICROCLIMATE IN THE CENTRE OF SMALL SQUARE SHELTERED PLOTS

J.C. ARGETE* and J.D. WILSON

Department of Geography, University of Alberta, Edmonton, Alberta T6G 2H4 (Canada)

(Received November 16, 1988; revision accepted February 13, 1989)

ABSTRACT

Argete, J.C. and Wilson, J.D., 1989. The microclimate in the centre of small square sheltered plots. Agric. For. Meteorol., 48: 185–199.

The difference in microclimate between the centre of a small square sheltered field and the undisturbed flow was examined experimentally as a function of atmospheric stability for two plot sizes $D/H = 8, 16$ (where D is the plot side length and H is the windbreak height) and two values of the height to roughness length ratio $H/z_0 = 25, 200$. Following McNaughton (1988), we isolated the short-term aerodynamically induced microclimate change by measuring the short-term changes in the mean equivalent temperature $\bar{T}_{eq}$ (a measure of the total heat content of the air). In the small plot, $\bar{T}_{eq}$ exceeded the undisturbed value by as much as $\sim 5\, T^*_{eq}$ (where T^*_{eq} is the equivalent temperature scaling parameter, determined essentially by the net radiation and friction velocity) during the day, with a converse effect of comparable magnitude occurring at night (i.e., reduction of the equivalent temperature in the small plot at night by an amount of order $5\, T^*_{eq}$). In contrast, the effect in the centre of the large plot was opposite in sign (by day and by night) to the changes observed in the small plot and smaller in magnitude. Hence, it is concluded that one may obtain a microclimatic benefit (increased temperature over most of the plot area) only by using a small plot size ($D/H \lesssim 10$).

INTRODUCTION

Figure 1 is a photograph of a small (10×10 m) plot surrounded by a porous windbreak. This paper will address the question: How does the microclimate within such a plot differ from that of the undisturbed flow? In particular, is it warmer or cooler in the plot? Drier or more humid? The mean wind in the plot will be reduced (see van Eimern et al., 1964), but is there an increase in the turbulence of the wind?

Why might one be interested in answering these questions? It is not uncommon to see the use of windbreak networks in agriculture, either in the context

*Present address: Department of Meteorology and Oceanography, University of The Philippines, Diliman, Quezon City, The Philippines.

0168-1923/89/$03.50

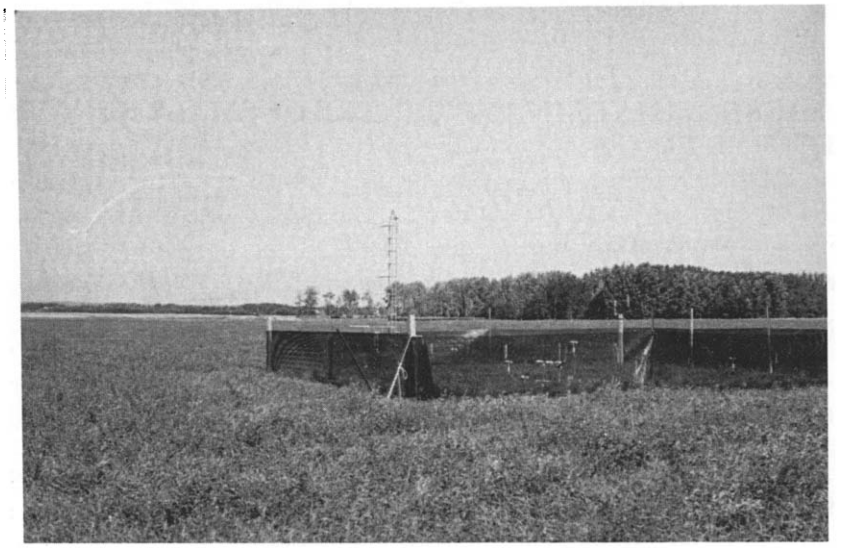

Fig. 1. A square plot of size 10×10 m enclosed by a windbreak of height $H = 1.25$ m and porosity $\phi = 45\%$.

of research to examine the potential benefits of shelter (e.g., Ogbuehi and Brandle, 1981) or in actual operation. Leaving aside the question of whether there may be a benefit (say, in increased yield or reduced time to harvest), the authors' impression is that there is confusion as to whether a benefit, if attained, is due to wind reduction, altered plot temperature, altered humidity and/or evapotranspiration rate, or some combination of these effects.

The questions posed above are incomplete when examined from the meteorologist's perspective. By asking if it is warmer in the plot, do we mean warmer on a seasonal, daily or an hourly basis and do we wish to include or exclude the (potential) effects of a response of a sheltered crop? For example, over a period of a month from establishing the shelter, the sheltered crop might develop a larger leaf area which may then feed back to result in a microclimate different from what we would observe under the same meteorological conditions with a uniform crop.

In this paper, we concentrate on short-term (of the order of 30 min average) changes which are entirely aerodynamic in origin (i.e., at least approximately independent of the nature of the sheltered crop). On the basis of field experiments, we will provide a partial answer to the questions posed above. The theory and background section outlines a dimensionless formulation for the description of changes in the mean equivalent temperature, $\overline{T}_{eq}$, which has been chosen as an unambiguous indicator of short-term microclimatic change. The experiments and analysis procedure section describes the experiments, and the results and discussion section gives and interprets our findings.

THEORY AND BACKGROUND

The adoption of equivalent temperature as a useful indicator of the windbreak aerodynamic effect

Following McNaughton (1988), who has carried out experiments along the lines of ours, but using long straight fences, we make the assumption that if we erect a porous fence around a plot and immediately measure (over say 30 min) the surrounding microclimate, the sum

$$Q^* - Q_G = Q_{H0} + Q_{E0} \tag{1}$$

(where the symbols represent the surface values of the net radiation and the soil, sensible and latent heat flux densities, respectively) is spatially uniform at a suitably uniform site, i.e., unaffected by the introduction of the windbreak. This is a reasonable assumption, at least if the shadow cast by the fence is not long, since the incoming short- and long-wave fluxes will be essentially unaffected by the fence*, as will the surface albedo and emissivity, and since the surface temperature changes will be small (a few degrees at most), the long-wave loss will be little altered by the presence of the fence. Again, it is worth stressing the short-term period under consideration, whereby we exclude the possibility of longer term crop response.

Now, if $Q^* - Q_G$ is spatially uniform, then so is the surface source strength for total thermodynamic energy, $Q_{H0} + Q_{E0}$, the sum of the rates of influx to the atmosphere of sensible and latent heat. This implies that any alteration in the concentration of thermodynamic energy in the air stream, which is measured by the equivalent temperature

$$T_{eq} = T + \frac{e}{\gamma} \tag{2}$$

(where T is the temperature, e is the vapour pressure, γ is the psychrometric constant and T_{eq} is the temperature the air would attain if all its latent heat was converted to sensible heat), must be entirely due to aerodynamic effects caused by the windbreak. Perhaps this statement will be clearer if we write down the K-theory model for the vertical transport of thermodynamic energy (which we will adopt as accurate in the upstream equilibrium flow, but as having only interpretative value in the disturbed region of the flow)

---

*One of the reviewers suggested that we comment on the likely effect of the presence of the fence upon the incoming long-wave radiation. A simple calculation for the location $x/H = 1$ using the appropriate view factors (Sparrow and Cess, 1978) indicates that the effect on incoming long-wave $L\downarrow$ is unlikely to exceed 10%. Then, provided $L\downarrow$ is itself a relatively small component of the radiation balance (i.e., given a strong solar component) the radiative influence of the fence should be unimportant. However, for nocturnal conditions, the radiative influence of the fence could be important.

$$Q_H + Q_E = -\rho c_p K \frac{\partial \overline{T}_{eq}}{\partial z} \quad (3)$$

where K is the eddy diffusivity, which we assume to take the same value for heat transport and vapour transport over the entire range of stability [this assumption is supported by the findings of Dyer and Bradley (1982) for unstable stratification and of Webb (1970) for stable stratification]. The implication of eq. 3 is that the distribution of $\overline{T}_{eq}$ is controlled by aerodynamic factors (accounted for by K in this model) and by the surface rate of input of thermodynamic energy. This remains true even though eq. 3 does not rigorously describe disturbed flow about the windbreak.

What would a knowledge of changes in $\overline{T}_{eq}$ tell us about changes in $\overline{T}$ and $\bar{e}$? In a dry system ($Q_{E0}=0$) $\Delta\overline{T}_{eq}=\Delta\overline{T}$, while in a (perhaps unattainable) system in which $Q^*-Q_G=Q_{E0}$, the change in equivalent temperature is entirely due to altered vapour density. Under intermediate conditions, the proportions of $\Delta\overline{T}_{eq}$ made up by $\Delta\overline{T}$ and $\Delta\bar{e}/\gamma$ are related to the value of the surface Bowen ratio, $B=Q_{H0}/Q_{E0}$. For practical purposes, values of shelter-induced changes in the equivalent temperature give an upper limit to the short-term temperature change which might be obtained.

Review of key features of flow about a straight porous windbreak

Reviews of the main features of the mean and turbulent velocity fields are given by van Eimern et al. (1964), Plate (1971) and Heisler and deWalle (1988). McNaughton (1988) reviews knowledge of the windbreak effect on both wind and microclimate.

Momentum is removed from the flow at the windbreak. This causes a mean velocity deficit both downstream and for a shorter range upstream. The degree and areal extent of wind reduction depend on many factors; however, the maximum value of the fractional mean velocity reduction is about

$$\Delta\bar{u}/\bar{u}_0 = 1.0/(1.0+2.0k_r)^{0.8} \quad (4)$$

where k_r is the pressure loss or resistance coefficient of the windbreak. This coefficient is defined as the ratio of the pressure drop across a section of the material set up to block a wind tunnel to the dynamic pressure scale, ρu^2. The estimation or measurement of k_r is straightforward.

Immediately above the fence is a sharp and shallow zone of increased velocity (necessary to ensure an invariant lateral mass flux). The ratio $\bar{w}/\bar{u}$ is small. Between the speed up and the velocity deficit region is a region of very strong wind shear, $\partial\bar{u}/\partial z$, relative to the same height in the approach flow. The action of the shear stress, $\overline{u'w'}$, itself increased in this region, upon this augmented wind shear leads to an increased rate of conversion of mean flow kinetic energy to turbulent kinetic energy. The consequence is a spreading zone of increased

turbulence (relative to the approach flow). The turbulent convection of horizontal momentum back from the speed up region to the decelerated region causes a fairly prompt recovery of the mean velocity field.

The fluctuating drag on the windbreak converts mean kinetic energy (MKE) to turbulent kinetic energy (TKE) and also takes kinetic energy from the relatively large scale eddies and passes this to very small (wake) scales of turbulence. In spite of the strong production of TKE at the windbreak, observations in the lee of straight porous fences (Raine and Stevenson, 1977; Wilson, 1987) show a zone of reduced TKE in the near lee, bounded from above by the zone of increased turbulence created by advection and diffusion of turbulence away from the region of increased shear production. It is likely that the existence of this quiet zone is a consequence of very rapid dissipation of the energy of the very small scales of motion and the strong extraction at the fence of energy from the larger scales of motion.

Dimensionless formulation

For clarity, let us begin by discussing the situation of an extensive spatially uniform ground-level source (of strength Q_c) of a passive tracer whose mean concentration is $\bar{c}(x,y,z)$. Assume neutral stratification. Then it is intuitively reasonable to expect that, all other things being held constant, if the source strength Q_c is doubled, all values of $\bar{c}(x,y,z)$ (and therefore differences in $\bar{c}$ between the undisturbed flow and a location in a sheltered plot) will also be doubled. Similarly, if we were to keep everything constant except for the friction velocity, u_*, which we (for argument's sake) halve, all values of $\bar{c}$ will again double since all emitted tracer now goes into half the volume of air, all wind speeds $\bar{u}$ (being proportional to u_*) having been halved. Thus, the dimensionless quantity $u_*\bar{c}/Q_c$ should be insensitive to changes in u_* and Q_c, but not necessarily other variables such as the surface roughness length z_0, the plot dimensions, fence height, etc.

For these reasons, it is convenient to define a dimensionless measure of the change in equivalent temperature

$$X=\frac{u_*\Delta\overline{T}_{eq}}{-\rho c_p(Q_{H0}+Q_{E0})}=\frac{\Delta\overline{T}_{eq}}{T^*_{eq}} \tag{6}$$

where $\Delta\overline{T}_{eq}$ is the difference (undisturbed−plot) in equivalent temperature and T^*_{eq} is the equivalent temperature scale

$$T^*_{eq}=-\frac{Q_{H0}+Q_{E0}}{\rho c_p u_*} \tag{7}$$

A full dimensional analysis allowing arbitrary surface and crop type, micrometeorological conditions, plot geometry, fence type and height would indicate the functional dependence of X to be

$$X=F\left(\frac{x}{H},\frac{y}{H},\frac{z}{H},\frac{L}{H},\frac{z_0}{H},\frac{D}{H},\phi,\beta\right) \tag{8}$$

where H is the height of the fence of uniform porosity ϕ, L is the Monin–Obukhov length, z_0 is the roughness length, D/H is the fence side length to height ratio (or the aspect ratio) and β is the wind direction. We have assumed the Reynolds number $\bar{u}(h)\delta/\nu$ to be so large as to render the flow insensitive to changes in that number.

There are several approaches to the determination of the actual dependency of X upon the controlling variables — field experimentation, wind tunnel experimentation and numerical simulation. In the experiments to be described in the following section, we have examined the dependence of X upon some members of the set of controlling variables. Our interpretation of the experimental data is necessarily primitive; this is a strongly disturbed, three-dimensional, stratified flow.

EXPERIMENTS AND ANALYSIS PROCEDURE

Equipment

Horizontal wind speed was measured with lightweight cup anemometers. Temperature and vapour pressure were measured with a set of eight shielded and ventilated electronic wet- and dry-bulb psychrometers built for the experiments. The sensing element was a 1N270 germanium diode operating in constant current mode.

The diode sensors were mounted in a PVC tube (internal diameter 2.54 cm) in a layout similar to that described by Black and McNaughton (1971). A single shield composed of a cylinder of polyurethane foam (wall thickness 0.7 cm) wrapped with reflectorized sheet was placed over the sensing head, which was ventilated at a rate slightly exceeding 5 m s^{-1}. The diode sensors were individually calibrated in a temperature-controlled water bath. In operation in the laboratory, eight psychrometers exhibited a range in dry- and wet-bulb temperature of $\pm 0.05\,^{\circ}C$ and agreed satisfactorily with a standard psychrometer.

In the field, frequent comparisons were made by placing all psychrometers together at $z=1$ m with intakes all within a cross-stream distance of 0.5 m and facing into the wind. Uniformity was not as good as in the laboratory, presumably due to variable radiation errors. On the basis of these comparisons, corrections were applied to the measured data, but undoubtedly some of the scatter in our experimental results is due to measurement error.

Site and experimental set-up

A series of experiments was conducted at two sites at the University of Alberta Farm, Ellerslie, Alberta. The first experiment (E1 hereafter) was carried out on 2–21 August 1986, over a large tract of land ($\sim$500 m radius), uniformly covered with alfalfa $\sim$25 cm tall. The second experiment (E2) was carried out on 25 April–26 May 1987, over a field ($\sim$1 km southwest of the first site) covered with 5-cm alfalfa stubble. The University Farm is relatively flat, with an estimated slope of $<1\%$.

A 5.5-m lattice-type tower was instrumented with five cup anemometers [z(m) = 0.61, 1.10, 2.10, 3.55, 5.50] and four diode psychrometers [z(m) = 0.61, 1.10, 2.10, 5.50]. These provided values of $\bar{u}(z)$, $\overline{T}(z)$, *and* $\overline{T}_w(z)$ to be used in determining the wind and temperature profiles of the approach flow.

The plot was $\sim$20 m distant from the tower. A plastic fence with a height $H = 1.25$ m, a porosity [manufacturer's (The Tensar Corporation, 2489 North Sheridan Way, c/o Gulf Canada Research Centre, Mississauga, Ontario, Canada) specification] $\phi = 45\%$ and a resistance coefficient $k_r = \Delta p/\rho u^2$ (determined by wind tunnel trial) was put up around a 10×10-m plot to give $D/H = 8$. The plot dimensions were occasionally doubled to give $D/H = 16$. The plot centre was instrumented with a cup anemometer and a psychrometer mounted on tripods at $z/H = 0.5$ or 0.25, equivalent to the level of the lowest anemometer and psychrometer on the tower. A wind vane was set up on an upwind post supporting the fence.

Turbulence measurements were taken during the second experiment using two single-axis sonic anemometers (Campbell Scientific Inc., Logan, UT, U.S.A.): one upwind and the other at the plot centre, both at $z/H = 0.25$.

Signals were routed to a small trailer and sampled continuously by a CR-7 (Campbell Scientific Inc., Logan, UT, U.S.A.) data logger. Digitized signals were transmitted to an IBM-PC. A compiled BASIC program calculated instantaneous vapour pressures and equivalent temperatures from sampled wet- and dry-bulb temperatures and stored averages. Each run lasted 15 min.

Using the displacement heights $d_{E1} = 15$ cm and $d_{E2} \cong 0$, values of the surface roughness lengths $z_{0(E1)} = 0.05$ m and $z_{0(E2)} = 0.0063$ m were determined graphically from the wind profiles of near-neutral runs.

Methods of analysis

From the measured profiles of windspeed, temperature and humidity, we calculated profiles of the mean virtual temperature, $\overline{T}_v$, and the mean equivalent temperature, $\overline{T}_{eq}$. By comparing the shapes of these profiles with standard profiles for uniform terrain, we deduced the values of the fluxes and the related

scaling variables. Our procedure is similar to that described by Nieuwstadt (1978).

Determination of u_*, T^*, T^*_{eq}

We adopted the standard profile formulation (Paulson, 1970)

$$\bar{u}(z)=\frac{u_*}{k}\left[\ln\frac{z}{z_0}-\psi_M\left(\frac{z}{L}\right)\right] \tag{9}$$

$$\overline{T}(z)-\overline{T}_0=\frac{T^*}{k}\left[\ln\frac{z}{z_0}-\psi_H\left(\frac{z}{L}\right)\right] \tag{10}$$

$$\overline{T}_{eq}(z)-\overline{T}_{eq0}=\frac{T^*_{eq}}{k}\left[\ln\frac{z}{z_0}-\psi_H\left(\frac{z}{L}\right)\right] \tag{11}$$

where k is von Karman's constant (we used $k=0.4$) and

$$T^*=-\frac{Q_H}{\rho c_p u_*}$$

is the scaling temperature analogous to T^*_{eq}. The diabatic correction factors were chosen to be

(1) Unstable stratification (Dyer and Bradley, 1982)

$$\psi_M=2\ln[\tfrac{1}{2}(1+x)]+\ln[\tfrac{1}{2}(1+x^2)]-2\arctan x+\frac{\pi}{2} \tag{13}$$

$$x=\Phi_M^{-1}=\left(1-28\frac{z}{L}\right)^{\frac{1}{4}} \tag{14}$$

$$\psi_H=2\ln[\tfrac{1}{2}(1+y)] \tag{15}$$

$$y=\Phi_H^{-1}=\left(1-14\frac{z}{L}\right)^{\frac{1}{2}} \tag{16}$$

(2) Stable stratification (Webb, 1970)

$$\psi_M=\psi_H=-5\frac{z-z_0}{L} \tag{17}$$

To allow for the influence of moisture upon buoyancy, we used a definition of the Monin–Obukhov length using the virtual temperature scale T^*_v rather than T^*

$$L=u_*^2 T_0/kgT^*_v \tag{18}$$

The standard virtual temperature profile was taken to be analogous to eq. 10, namely

$$\overline{T}_{\mathrm{v}}(z)-\overline{T}_{\mathrm{v0}}=\frac{T_{\mathrm{v}}^{*}}{k}\left[\ln\frac{z}{z_0}-\psi_{\mathrm{H}}\left(\frac{z}{L}\right)\right] \tag{19}$$

The parameter determination was carried out by fitting the measured profiles to the empirical profile relationships using the minimum residual procedure. One of the measured velocities (virtual temperatures) is designated the reference value, say at height $z_u(z_T)$, from which measured differences are formed

$$\begin{aligned}\Delta\bar{u}_{\mathrm{m},j}&=\bar{u}_{\mathrm{m},j}(z_j)-\bar{u}_{\mathrm{m}}(z_u) \qquad j=1\ldots n_u-1\\ \Delta\overline{T}_{\mathrm{vm},k}&=\overline{T}_{\mathrm{vm},k}(z_k)-\overline{T}_{\mathrm{vm}}(z_T) \quad k=1\ldots n_T-1\end{aligned} \tag{20}$$

where $n_u(n_T)$ is the number of velocity (temperature) measurement levels. Corresponding theoretical differences $\Delta\bar{u}_{\mathrm{t},j}$,$\Delta\overline{T}_{\mathrm{vt}},k$ were also formed over the same height intervals from eqs. 9 and 19. An iterative procedure was used to systematically scan through possible pairs of u_*,T_{v}^{*}, with the optimal values formed from the condition that the function ϕ reaches a minimum

$$\phi(u_*,T_{\mathrm{v}}^{*})=g_u\phi_u+g_{T_{\mathrm{v}}}\phi_{T_{\mathrm{v}}} \tag{21}$$

where

$$\phi_u=\sum_{j=1}^{n_u-1}(\Delta\bar{u}_{\mathrm{m},j}-\Delta\bar{u}_{\mathrm{t},j})^2 \tag{22}$$

$$\phi_{T_{\mathrm{v}}}=\sum_{k=1}^{nT-1}(\Delta\overline{T}_{\mathrm{vm},k}-\Delta\overline{T}_{\mathrm{vt},k})^2 \tag{23}$$

and g_u and $g_{T_{\mathrm{v}}}$ are weight factors chosen to properly reflect the relative size of the measurement errors in temperature and humidity. The value of L is fixed from the u_* and T_{v}^{*} values found from the loop. Similar iterations for eqs. 10 and 11 determine the values of T^{*},T_{eq}^{*} associated with the minima of ϕ_T,$\phi_{T_{\mathrm{eq}}}$ as in eqs. 22 and 23.

Criteria for selection of acceptable runs

Any run for which (a) the wind blew from plot to tower and/or (b) the theoretical and measured profiles disagreed very markedly was discarded. The remaining runs were accepted if (i) $|T_{\mathrm{eq}}^{*}|>0.15\,^{\circ}\mathrm{C}$; (ii) $\bar{u}(z_1)>0.6\,\mathrm{m\,s^{-1}}$; and (iii) $|T^{*}|>0.08\,^{\circ}\mathrm{C}$. Criterion (ii) ensures that runs subject to cup stoppages are rejected, and (i) and (iii) ensure that temperature differences are large enough to be measurable.

Comparison of profile-derived and directly-measured $\mathrm{Q}_H+\mathrm{Q}_E$

The flux of total energy $(Q^{*}-Q_{\mathrm{G}})$ [$\mathrm{W\,m^{-2}}$] was obtained from independent measurements of Q^{*} using a net radiometer and Q_{G} with a soil heat flux plate.

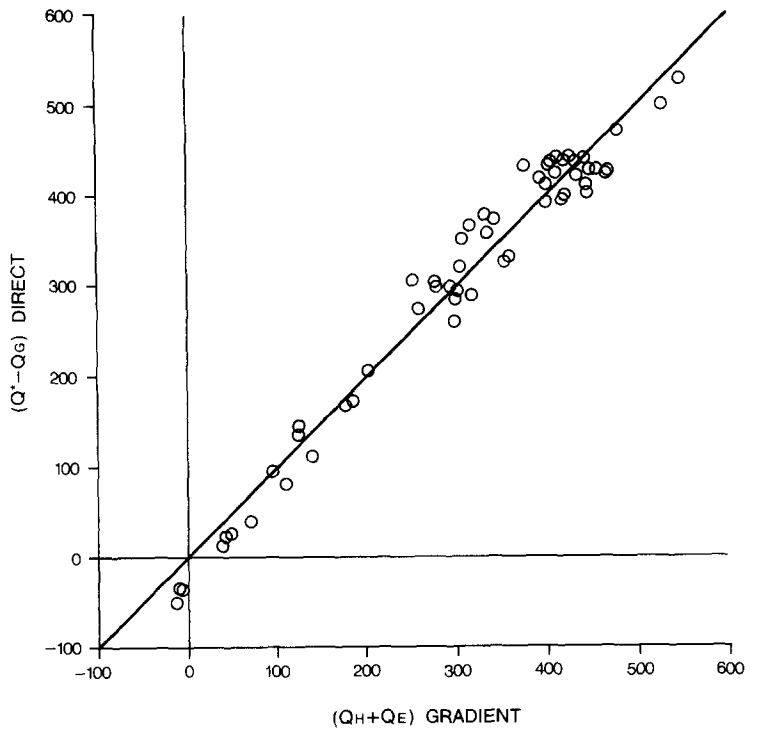

Fig. 2. Comparison of the total energy flux, $Q_H + Q_E$ (W m^{-2}), determined by the gradient method and $Q^* - Q_G$ directly measured. The diagonal is the 1:1 line.

The corresponding profile-derived flux $(Q_H + Q_E)_{GRADIENT}$ was calculated based on eq. 7 using the scaling variables as determined in this section. Figure 2 shows reasonably good agreement between the fluxes determined from the two methods.

RESULTS AND DISCUSSION

Identification of quiet and turbulent zones

It is useful to show the existence of the quiet and turbulent zones for the two square plots. A convenient measurement of the turbulence is σ_w, the standard deviation of the vertical velocity fluctuation. Figure 3 shows the observed fractional change in σ_w, $\Delta\sigma_w/\sigma_{wo}$ (where σ_{wo} is the upstream value and a positive value implies decreased turbulence in the plot). There is a strong contrast of values between the small and large plots. For the entire range of atmospheric stability shown, the middle of the large plot ($D/H=16$, $x/H=8$) was consistently in the turbulent zone. The centre of the small plot ($D/H=8$, $x/H=4$)

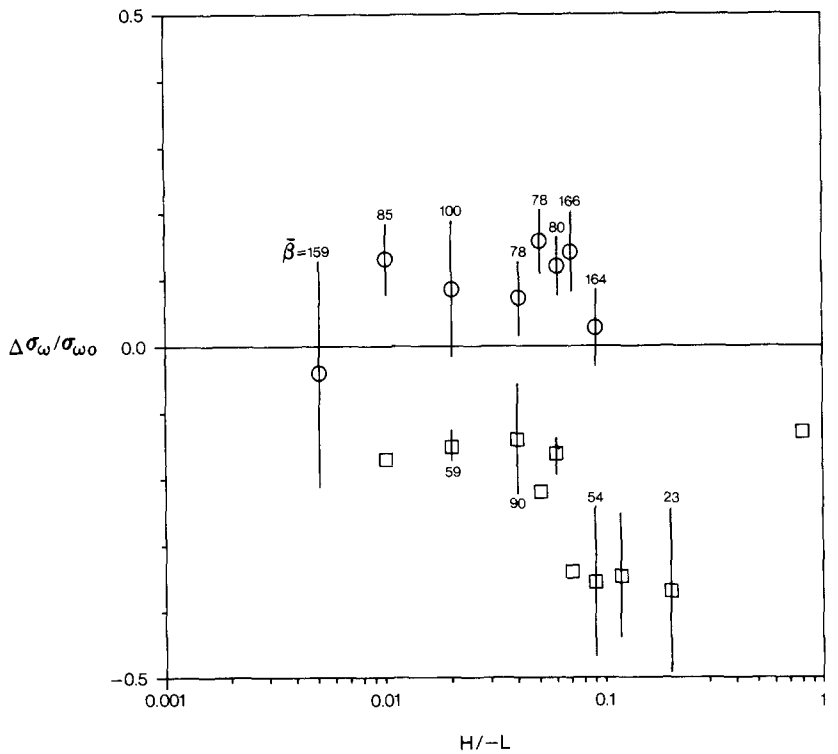

Fig. 3. Observed changes in the standard deviation of the vertical velocity for unstable stratification with $z/H=0.25$ and $H/z_0=200$. ○, $D/H=8$; □, $D/H=16$. Here and elsewhere, a symbol ∅ (etc.) represents the mean of a group of observations falling within a narrow stability range ± the standard error of that mean. Single observations appear without an error bar.

was in the quiet zone most of the time, except in cases when the mean wind direction, $\bar{\beta}$, was far from normal ($\bar{\beta}=90$) to the fence. This is probably a manifestation of the corner effect observed by Gandemer (1979) which exacerbates turbulence generation by the fence and in effect shortens the horizontal extent of the quiet zone.

Modification of the equivalent temperature

It will be noted that for daytime runs when conditions are generally lapse (unstable stratification) and the total energy flux (Q_H+Q_{LE}) is positive, $T^*_{eq}<0$ and $H/L<0$. At night when stable stratification prevails so that the fluxes of sensible and latent heat are both directed downwards, T^*_{eq} turns positive with H/L. Positive values of X are therefore indicative of warming in $\overline{T}_{eq}$ in the plot during the day and cooling at night.

Figures 4 and 5 present the observed changes in equivalent temperature in

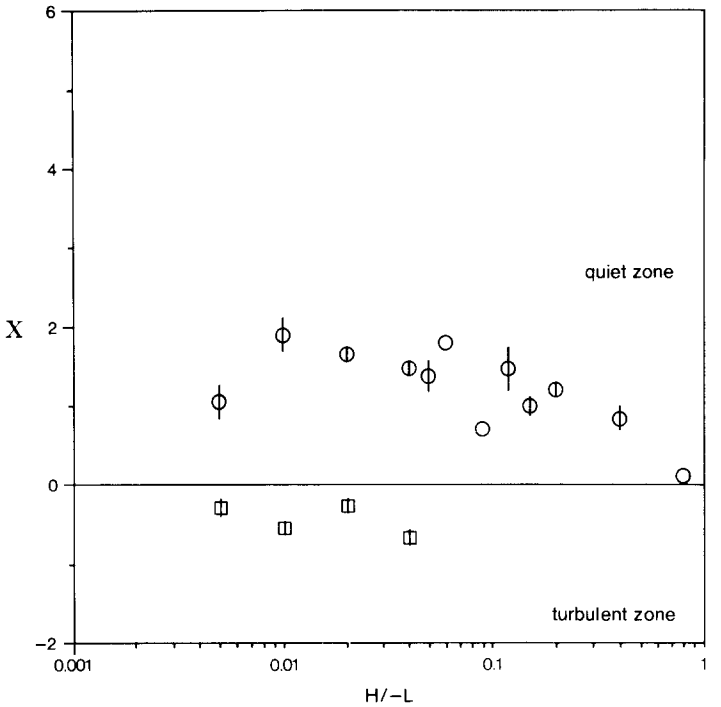

Fig. 4. Observed modification of the equivalent temperature for unstable stratification with $z/H=0.5$, $H/z_0=25$. Modification is plotted as $X=\Delta\overline{T}_{eq}/T^*_{eq}$ with positive values in this case meaning increased $\overline{T}_{eq}$ within the plot. ○, $D/H=8$; □, $D/H=16$.

unstable stratification. Two points are immediately clear: (i) there is daytime warming in $\overline{T}_{eq}$ in the centre of the small plot; (ii) there is daytime cooling in the centre of the large plot.

It is also clear that the magnitude of the increase in $\overline{T}_{eq}$ within the small plot is much larger for the case $[z/H=0.25, H/z_0=200]$ than for the case $[z/H=0.5, H/z_0=25]$.

As $|\frac{H}{L}| \to \infty$, the shelter effect diminishes (observed, at fixed x/H).

McNaughton (1988; Fig. 5) presents a streamwise profile of $X=\Delta\overline{T}_{eq}/T^*_{eq}$ measured at $z/H=0.15$ behind a straight 50% porous fence erected in a field of grazed pasture. The height to roughness length ratio ($H/z_0=150$) and the height to stability length ratio ($H/L=-0.05$) for McNaughton's data allow comparison with the data given in our Fig. 5. At $x/H=4$, corresponding (at least for flow normal to the plot sides) to the centre of our small plot, McNaughton reports $X=3.8$. The close similarity between this value and our measurements suggests that perhaps the same mechanisms dominate both of these flows and that the difference in geometry (straight fence versus square plot)

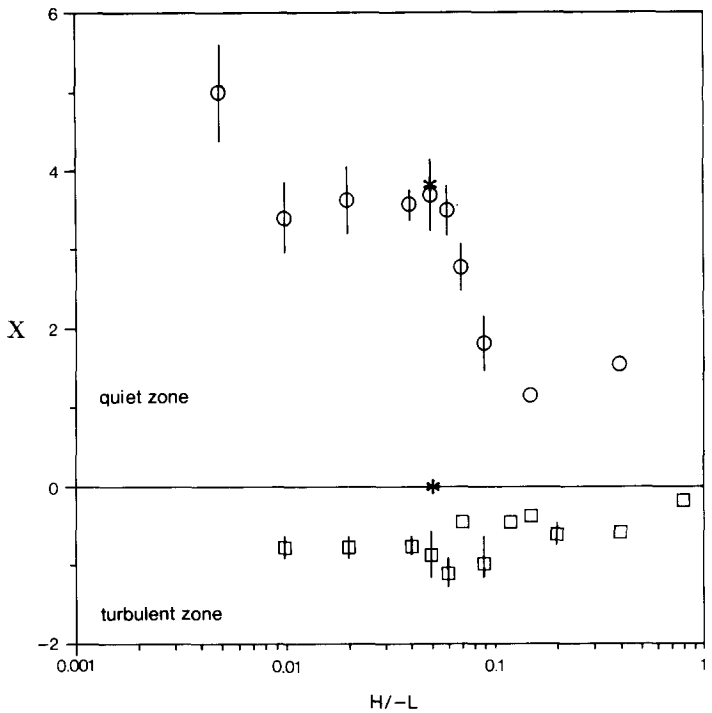

Fig. 5. Observed modification of the equivalent temperature for unstable stratification with $z/H=0.25, H/z_0=200$. ○, $D/H=8$; □, $D/H=16$. The * values are data from McNaughton (1988) at distances $x/H=4$ (upper star) and $x/H=8$ (lower star) behind a straight fence; values of $(z/H, H/z_0)$ for the McNaughton data were 0.15, 150.

is of secondary importance. However, it should be borne in mind that there are several differences in the relevant non-dimensional ratios pertaining to the two experiments. At $x/H=8$, corresponding to the centre of our large plot, McNaughton reports $X\approx 0$, while we have measured $X\approx -\frac{1}{2}$. Again, there seems to be consistency as to the range of the modification of microclimate behind the different types of shelter flow.

We can give only a qualitative explanation for the existence of the warm and cool zones (which coincide with the quiet and turbulent zones). The surface energy flux is by assumption uniform. The effective eddy diffusivity is decreased (increased) in the quiet (turbulent) zone in the middle of the small (large) plot. Hence, to transfer the necessary flux, the gradient $\partial \overline{T}_{eq}/\partial z$ must be more negative in the small plot. Since the windbreak can have no effect far aloft, the increased gradient must come about by an increase in the equivalent temperature near the ground.

Measurements under stable stratification ($H/L>0$) are shown in Fig. 6. As stated earlier, the assumption of a spatially uniform thermodynamic energy flux at ground is less reasonable for nocturnal conditions. As in all experimen-

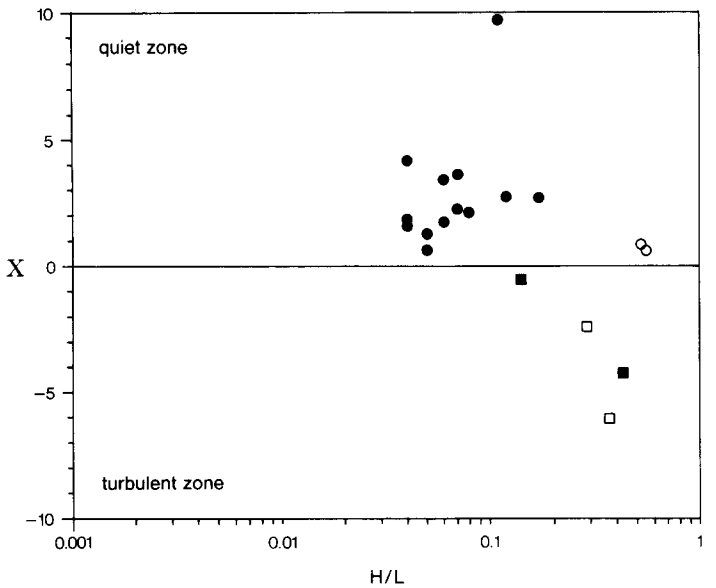

Fig. 6. Observed modification of the equivalent temperature in stable stratification. ●, ■ $D/H=8, 16$ ($z/H=0.25, H/z_0=200$); ○, □ $D/H=8, 16$ ($z/H=0.5, H/z_0=25$).

tal studies of stably stratified layers, aside from the difficulty of dealing with a process involving intermittency, the major constraint is instrumentation, hence the scarcity of acceptable runs. Nevertheless, the figure indicates that the centre of the small plot is in the quiet zone (cooling in $\overline{T}_{eq}$) and that of the large plot is in the turbulent zone (warming in $\overline{T}_{eq}$). The observation for the large plot proved to be contrary to our expectation that under stable conditions the quiet zone would extend to the centre of the big plot at $x/H \approx 8$. Apparently, the fence-generated turbulence, although small in magnitude, becomes significant given the relative calm prevailing upwind. The dependence of X on H/L, z/H and H/z_0 cannot be inferred from the available data.

SUMMARY

Observations have shown that at the centre of a small square plot ($D/H=8$) there is daytime warming and night-time cooling in the mean equivalent temperature $\overline{T}_{eq}$ relative to the same height upstream. This might represent a benefit for crop growth (in some circumstances). However, the opposite effect is noted in plots of size $D/H=16$, implying that the (possible) benefit may be obtained only by using very small plots. The existence of warming/cooling is linked to the existence of increased or reduced turbulence of the vertical wind. The magnitude of the effect, besides depending on plot size, depends on many other factors (including fence height, atmospheric stability, surface roughness

length, measurement height). The largest alterations observed were $\Delta\overline{T}_{eq} \sim 5T^*_{eq}$.

REFERENCES

Black, T.A. and McNaughton, K.G., 1971. Psychrometric apparatus for Bowen-ratio determination over forests. Boundary-Layer Meteorol., 2: 246–254.

Dyer, A.J. and Bradley, E.F., 1982. An alternative analysis of flux-gradient relationships at the 1976 ITCE. Boundary-Layer Meteorol., 22: 3–19.

Gandemer, J., 1979. Wind shelters. J. Ind. Aerodyn., 4: 371–389.

Heisler, G.M. and deWalle, D.R., 1988. Effects of windbreak structure on windflow. Agric. Ecosystems Environ., 22/23: 41–69.

McNaughton, K.G., 1988. Effects of windbreaks on turbulent transport and microclimate. Agric. Ecosystems Environ., 22/23: 17–39. Also published in: J.R. Brandle, D.L. Hintz and J.W. Sturrock (Editors), Windbreak Technology. Elsevier, Amsterdam.

Nieuwstadt, F., 1978. The computation of the friction velocity u_* and the temperature scale T_* from temperature and wind velocity profiles by least-square methods. Boundary-Layer Meteorol., 14: 235–246.

Ogbuehi, S.N. and Brandle, J.R., 1981. Influence of windbreak-shelter on soybean production under rainfed conditions. Agron. J., 73: 625–628.

Paulson, C.A., 1970. The mathematical representation of wind speed and temperature profiles in the unstable atmospheric surface layer. J. Appl. Meteorol., 9: 857–861.

Plate, E.J., 1971. The aerodynamics of shelterbelts. Agric. Meteorol., 8: 203–222.

Raine, J.K. and Stevenson, D.C., 1977. Wind protection by model fences in a simulated atmospheric boundary layer. J. Ind. Aerodyn., 2: 159–180.

Sparrow, E.M. and Cess, R.D., 1978. Radiation Heat Transfer. McGraw Hill, New York.

Van Eimern, J., Karschon, R., Razumova, L.A. and Robertson, G.W., 1964. Windbreaks and shelterbelts. WMO Tech. Note No. 59.

Webb, E.K., 1970. Profile relationships: the log-linear range and extension to strong stability. Q. J. R. Meteorol. Soc., 96: 67–90.

Wilson, J.D., 1987. On the choice of a windbreak porosity profile. Boundary-Layer Meteorol., 38: 37–49.